

# A Brighter Past: Galaxy Luminosity Function At High Redshifts

Asantha Cooray

*Department of Physics and Astronomy, University of California, Irvine, CA 92697*  
*E-mail: acooray@uci.edu*

24 December 2018

## ABSTRACT

Using the conditional luminosity function — the luminosity distribution of galaxies in a dark matter halo as a function of the halo mass — we present an empirical model to describe the redshift evolution of the rest B-band galaxy luminosity function (LF). The model is compared to measured LFs out to a redshift of 3.5, including LFs of galaxy types separated to red and blue galaxies. The increase in the number density of luminous galaxies, at the bright-end of the LF, can be explained as due to a brightening of the luminosity of galaxies present in dark matter halo centers, relative to the luminosity of central galaxies in similar mass halos today. The lack of strong evolution in the faint-end of the LF, however, argues against a model involving pure luminosity evolution at all halo mass scales. The increase in luminosity at the bright-end compensates the rapid decline in the number density of massive halos as the redshift is increased. The decline in group to cluster-mass dark matter halos out to a redshift of  $\sim 2$  is not important as the central galaxy luminosity flattens at halo masses around  $10^{13} M_{\odot}$ . At redshifts  $\sim 2$  to 3, however, the density of bright galaxies begins to decrease due to the rapid decline in the number density of dark matter halos at mass scales around and below  $10^{13} M_{\odot}$ . We compare our predictions to the UV LF of galaxies at redshifts 3 to 6 and the galaxy clustering bias measurements at redshifts  $\sim 3$ , and use our models to establish the dark matter halo mass scales of galaxies observed at high redshifts. In general, to explain high-redshift LFs, galaxies in dark matter halos around  $10^{12} M_{\odot}$  must increase in luminosity by a factor of  $\sim 4$  to 6 between today and redshift of 6.

**Key words:** large scale structure — cosmology: observations — cosmology: theory — galaxies: clusters: general — galaxies: formation — galaxies: fundamental parameters — intergalactic medium — galaxies: halos — methods: statistical

## 1 INTRODUCTION

The luminosity function (LF) of field galaxies at the present day can be described using a simple empirical model that involves the dark matter halo mass function and the relation between central galaxy luminosity and the halo mass (Cooray & Milosavljevic 2005b; Cooray 2005). The model utilizes an approach based on the conditional luminosity function (CLF; Yang et al. 2003b, 2005), or the luminosity distribution of galaxies as a function of the halo mass, to construct the LF. The CLFs are basically an extension of the halo approach to galaxy statistics (Seljak 2000; Scoccimarro et al. 2001; Cooray et al. 2000; see, Cooray & Sheth 2002 for a review) where instead of the halo occupation number,  $\langle N_g \rangle$ , involving an average number of galaxies as a function

of the dark matter halo mass, we consider the number of galaxies as a function of the galaxy luminosity; thus, the CLF is the conditional halo occupation number,  $dN_g/dL$ . Other conditions of the halo occupation number has been suggested (such as the stellar mass in Zheng et al. 2004), but for comparison with observations, galaxy luminosity and type are considered here.

Note that the integral of the CLF over luminosity is the mean halo occupation number. As the halo occupation statistics are best described based on a division to central and satellite galaxies (Kravtsov et al. 2003), we also divide CLFs to central galaxies and satellites; central galaxies are assigned a log-normal distribution in the luminosity, centered around the mean central galaxy luminosity given the halo mass, and satellite galaxies are assigned a power-

law distribution. This empirical approach has the main advantage that it can elucidate important ingredients associated with the galaxy distribution. Statistical measurements from observations mostly include LFs and aspects involving galaxy clustering, such as the bias factor or the correlation length. Thus, we use CLFs to model same statistics here. Previous studies with the halo model to describe galaxy statistics concentrated primarily on average clustering properties (e.g., Seljak 2000; Scoccimarro et al. 2001; Cooray 2002; Berlind et al. 2003); for these statistics, one does not care about the conditional occupation number, either in luminosity or other galaxy property, but rather the average occupation number itself. The present method, however, improves previous attempts since one can now calculate both galaxy-property dependent statistics, such as the LF, while at the same time modeling conditional statistical measurements, such as clustering as a function of galaxy luminosity (e.g., Zehavi et al. 2004). Here, we will concentrate mainly on the galaxy LF at high redshifts.

The CLF approach to galaxy statistics has been used to explain why the LF can be described with the Schechter (1976) form of  $\Phi(L) \propto (L/L_*)^\alpha \exp(-L/L_*)$  (see, Cooray & Milosavljević 2005b). The main ingredient, in addition to the halo mass function, is the relation between central galaxy luminosity and the halo mass, hereafter called the  $L_c(M)$  relation. This relation, as appropriate for galaxies at low-redshifts, was established in Cooray & Milosavljević (2005a) from a combination of weak lensing (e.g., Yang et al. 2003a) and direct measurements of galaxy luminosity and mass in groups and clusters (e.g., Lin et al. 2004). The same relation has been established with a statistical analysis of the 2dFGRS  $b_J$ -band LF (e.g., Norberg et al. 2002) by Vale & Ostriker (2004) and, independently, by Yang et al. (2005) based on the group catalog. The shape of the  $L_c(M)$  relation, where luminosities grow rapidly with increasing mass but flattens at a mass scale around  $\sim 10^{13} M_\odot$  is best explained through dissipationless merging history of central galaxies. We refer the reader to Cooray (2005) for full details related to this empirical modeling approach, including an extension of this technique to describe statistics of galaxy types such as red (early-type) and blue (late-type) galaxies, when the galaxy sample is broadly divided in to two classes.

In addition to galaxy statistics today from wide-field redshift surveys such as the 2dF Galaxy Redshift Survey (2dFGRS; Colless et al. 2001) or the Sloan Digital Sky Survey (SDSS; York et al. 2000), various techniques, such as the Lyman drop-out method (e.g., Steidel et al. 1999), have now allowed the study of galaxy LF and other statistics on the galaxy distribution at high redshifts. While the LF of galaxies today can be described through the observationally established  $L_c(M)$  relation, it is also useful to understand the extent to which the same empirical approach can be applied at high redshifts. In return, using the measured galaxy LFs out to a redshift of 6, we can then extract information on how galaxy luminosities evolve as a function of redshift. The model allows one to address if the galaxy formation was efficient in the past and how galaxy properties are different when compared to properties today.

Here, we compare our predictions to the measured rest

frame B-band LF of galaxies, including red and blue galaxies, out to a redshift of 3.5 from Giallongo et al. (2005). We also make comparisons to rest-UV LFs of galaxies at redshifts 3 to 6 from Steidel et al. (1999) and Bouwens et al. (2004a). Note that the high redshift B-band LF of Giallongo et al. (2005) is constructed from observations made at a variety of wavelengths, but corresponding to B-band in the rest-frame. While previous studies have measured the redshift dependence of the LF, say in the K-band (e.g., Drory et al. 2003), given that the LF corresponds to different rest wavelengths as a function of redshift, any evolutionary aspects associated with galaxy properties, at a given wavelength, must be distinguished from evolutionary effects resulting from color differences. The B-band LFs of Giallongo et al. (2005) have the advantage that one can directly address how galaxy properties change with redshift at the same band, regardless of color differences.

The paper is organized as follows: In the next section, we will outline the basic ingredients in the empirical model for CLFs and how it is modified to model the LF at high redshifts. We refer the reader to Cooray (2005) and Cooray & Milosavljević (2005a) for detailed discussions related to this empirical modeling approach. In Section 3, we will describe the  $z$ -dependent LF and compare with measurements by Giallongo et al. (2005). We also compare our models to rest-UV LFs of galaxies between redshifts of 3 to 6, and galaxy clustering bias around the same redshift ranges. We conclude with a summary of our main results and implications related to the galaxy distribution at redshifts  $\sim 3$  to 6 in § 4. Throughout the paper, we assume cosmological parameters consistent with Giallongo et al. (2005) with  $\Omega_m = 0.3$ ,  $\Omega_\Lambda = 0.7$  and a scaled Hubble constant of  $h = 0.7$ , in units of  $100 \text{ km s}^{-1} \text{ Mpc}^{-1}$ . The matter power spectrum is normalized to a  $\sigma_8$ , rms fluctuations at  $8 h^{-1} \text{ Mpc}$  scales, of 0.84 consistent with WMAP data (Spergel et al. 2003).

## 2 CONDITIONAL LUMINOSITY FUNCTION: EMPIRICAL MODEL

In order to construct the redshift evolution of the luminosity function (LF), we follow Cooray & Milosavljević (2005b) and Cooray (2005). The conditional luminosity function (CLF; Yang et al. 2003b, 2005), denoted by  $\Phi(L|M, z)$ , is the average number of galaxies with luminosities between  $L$  and  $L + dL$  that reside in halos of mass  $M$  at a redshift of  $z$ . As in our application to 2dFGRS at  $z = 0$  (Cooray 2005), the CLF is separated into terms associated with central and satellite galaxies, such that

$$\begin{aligned} \Phi(L|M, z) &= \Phi_c(L|M, z) + \Phi_s(L|M, z) \\ \Phi_c(L|M, z) &= \frac{f_c(M, z)}{\sqrt{2\pi} \ln(10) \Sigma(z) L} \times \\ &\quad \exp \left\{ -\frac{\log_{10}[L/L_c(M, z)]^2}{2\Sigma^2(z)} \right\} \\ \Phi_s(L|M) &= A(M, z) L^{\gamma(M, z)}. \end{aligned} \quad (1)$$

Here  $L_c(M, z)$  is the relation between central galaxy luminosity of a given dark matter halo and its halo mass, taken

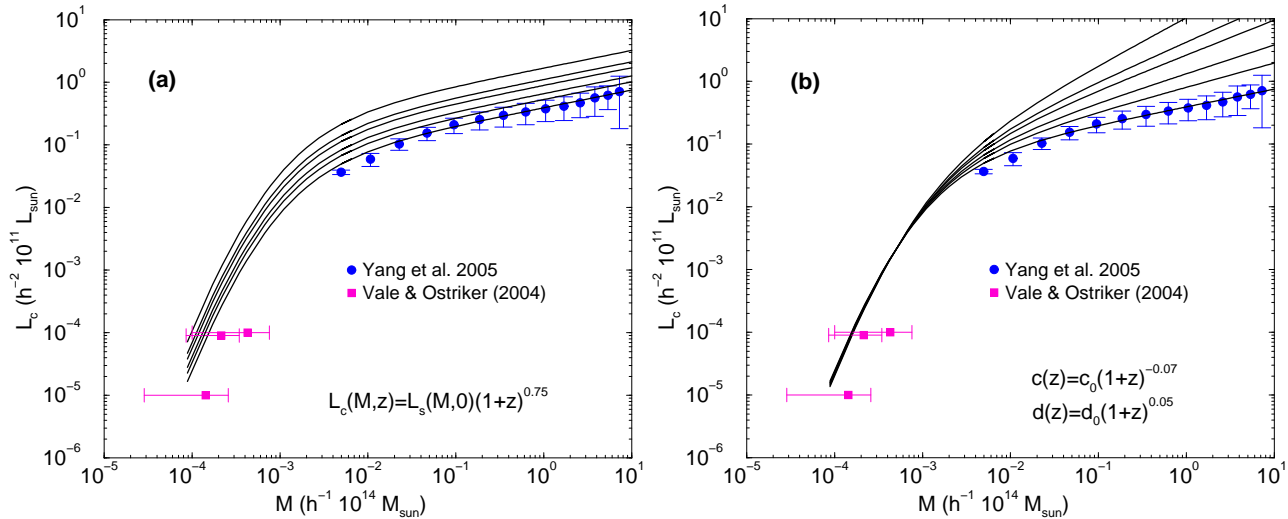


**Figure 1.** Central galaxy luminosity as a function of the halo mass as appropriate for 2dFGRS  $b_J$ -band. The data points at the low mass end are from Vale & Ostriker (2004; *squares*) while at the high end are from Yang et al. (2005). The solid curves are the relation as a function of redshift; from bottom to top in each of the two panels, the redshifts are 0, 0.5, 1, 2, 3, and 6, respectively. The relation at  $z = 0$  comes from Vale & Ostriker (2004) in the  $b_J$  band of 2dFGRS by converting the luminosity function to extract the plotted relation based on the sub-halo mass function. We use this relation to construct our the CLF, and include a scatter in this relation in our description of central galaxy CLFs.

to be a function of redshift, while  $\ln(10)\Sigma(z)$  is the dispersion in this relation, again a function of redshift.

The central galaxy CLF takes a log-normal form, while the satellite galaxy CLF takes a power-law form in luminosity. Such a separation describes the LF best, with an overall better fit to the data in the K-band as explored by Cooray & Milosavljević (2005b) and 2dFGRS  $b_J$ -band in Cooray (2005). Our motivation for log-normal distribution also comes from measured conditional LFs, such as galaxy cluster LFs that include bright central galaxies, where a log-normal component, in addition to the Schechter (1976) form, is required to fit the data (e.g., Trentham & Tully 2002). Similarly, the stellar mass function, as a function of halos mass in semi-analytical models, is best described with a log-normal component for central galaxies (Zheng et al. 2004). To simplify the modeling approach, we assume  $\Sigma(z) = \Sigma(0) = 0.17$ , and  $\gamma(M, z) = -0.5$ ; The value for  $\Sigma$  comes from a comparison to low-redshift LF in 2dFGRS (Norberg et al. 2002), while the latter ignores the mass dependence of the satellite luminosity distribution suggested in Cooray (2005). The relations  $f_c(M, z = 0)$ , as well as fractional relations, as a function of the halo mass, that were used to divide the galaxy sample to early- and late-type galaxies is described in Cooray (2005); we ignore any redshift dependences in these functions, and assume that regardless of the redshift, the fraction of of early-to-late type galaxies, in a halo of fixed mass, is same as the fraction of that halo mass today. Thus, the only redshift dependence in this model comes from any redshift dependence in the  $L_c(M, z)$  relation, and when describing satellites,  $L_{\text{tot}}(M, z)$ , the total luminosity of galaxies as a function of the halo mass, relation; the latter, however, is not an important ingredient

since the LF is primarily determined by statistics of central galaxies (Cooray & Milosavljevic 2005b; Cooray 2005).

## 2.1 Central Galaxy Luminosity-Halo Mass Relation

For  $L_c(M, z = 0)$  relation, here we make use of the relation derived in Vale & Ostriker (2004). These authors established this relation by inverting the 2dFGRS luminosity function given an analytical description for the sub-halo mass function of the Universe (e.g., De Lucia et al. 2004; Oguri & Lee 2004). We used this relation to describe the 2dFGRS  $b_J$ -band LF in Cooray (2005), and we will use the same relation, at  $z = 0$ , as an approximation to describe the B-band LF. The relation is described with a general fitting formula given by

$$L(M, z = 0) = L_0 \frac{(M/M_1)^a}{[b + (M/M_1)^{cd}]^{1/d}}. \quad (2)$$

For central galaxy luminosities, the parameters are  $L_0 = 5.7 \times 10^9 L_\odot$ ,  $M_1 = 10^{11} M_\odot$ ,  $a = 4.0$ ,  $b = 0.57$ ,  $c = 3.72$ , and  $d = 0.23$  (Vale & Ostriker 2004). For the total galaxy luminosity, as a function of the halo mass, we also use the fitting formula in equation (2), but with  $c = 3.57$ . As discussed in Cooray (2005), the overall shape of the LF is *strongly* sensitive to the shape of the  $L_c$ - $M$  relation, and it's scatter, and less on details related to the  $L_{\text{tot}}$ - $M$  relation.

To describe the redshift evolution, we consider two possibilities. First, we describe the high- $z$  LFs with  $L(M, z) = L(M, z = 0)(1+z)^\alpha$ . This is a scenario in where all luminosities either increase or decrease depending on the value and sign of  $\alpha$ , which we take to be mass independent. Such an evolution provides an acceptable description of the LFs

of Giallongo et al. (2005), though the increase in luminosity of galaxies in less massive dark matter halos overestimates the LF at the faint-end at high redshifts. At  $z \sim 6$ , this overestimate becomes significant and even the LF at the bright-end is overestimated relative to the UV LF measured by Bouwens et al. (2004a). A preferred description may be a case where low luminosity end of the  $L_c(M, z)$  relation remains independent of the redshift, while the bright-end increases with increasing redshift. To describe this behavior, we take parameters  $c$  and  $d$  in equation (2) to be dependent on the redshift with  $c(z) = c(z=0)(1+z)^\beta$  and  $d(z) = d(z=0)(1+z)^\eta$ , where  $\beta$  and  $\eta$  are taken to be free parameters.

In Figure 1, we show the  $L_c(M, z)$  relation as a function of the halo mass and for redshifts from 0 to 6. For comparison, we also show measurements from the 2dFGRS galaxy group catalog from Yang et al. (2005). In the left panel, we show the pure-luminosity evolution case with  $\alpha = 0.75$  and in the right-panel, we show the evolution of the bright-end with  $\beta = -0.07$  and  $\eta = 0.05$ ; These numerical values were selected based on a comparison to the high-redshift LFs of Giallongo et al. (2005).

Note that we are assuming here that the central galaxy luminosity of a given halo increases with redshift. This assumption does not violate the fact that the halo occupation number is not changing with redshift (e.g., Yan et al. 2003; Coil et al. 2004), since the integral of  $\Phi(L|M)$  over luminosities remain the same; all we have done is to shift the mean of the log-normal distribution that describes central galaxy luminosity distribution to a higher luminosity when compared to the value today. The fact that the halo occupation number is the same at high redshifts, when compared to today, should not be considered as a statement that galaxy properties do not change with redshift.

### 3 HIGH-REDSHIFT LUMINOSITY FUNCTIONS

Given our model for CLFs, we can now construct the LF, which is an average of CLFs over the halo mass distribution given by the mass function. Here, we use the Sheth & Tormen (1999; ST) mass function  $dn/dM$  for dark matter halos. This mass function is in better agreement with numerical simulations (Jenkins et al. 2001), when compared to the more familiar Press-Schechter (PS; Press & Schechter 1974) mass function. While there are differences in the ST mass function and the numerically simulated mass functions at the high mass end, these differences do not affect these results, since statistics of the LF at the present day are dominated by galaxies in halos around  $10^{13} M_\odot$ . Here, we make the assumption that the ST mass function is the corrected description for halo masses out to  $z \sim 6$  and above; any differences in the evolution of the mass function, relative to ST description, could affect our conclusions regarding luminosity evolution.

Given the mass function, the galaxy LF as a function of  $z$  is

$$\Phi_i(L, z) = \int_0^\infty \Phi_i(L|M, z) \frac{dn}{dM}(z) dM, \quad (3)$$

where  $i$  is an index for early and late type galaxies. The conditional luminosity function for each type involves the sum of central and satellites. To compare with Giallongo et al. (2005) measurements, we will plot these two divisions, as well as the sum separately for late-type (blue) and early-type (red) galaxies.

In Figure 2, we show the LF of galaxies at redshifts out to 3.5. In Figure 2(a), we present a comparison to a model of the  $z = 0$  LF of 2dFGRS data from Cooray (2005). In Figure 2(b), we assume no redshift evolution in the  $L_c(M, z)$  relation. The resulting LFs are then affected only by the redshift evolution of the dark matter halo mass function,  $dn/dm(z)$ . At low redshifts, the dark matter halo mass function evolves such that the number density of massive halos is rapidly decreasing while the density of halos at masses around and below  $\sim 10^{12} M_\odot$  is slightly increasing, relative to the mass function at  $z = 0$  (see, Reed et al. 2003). This evolution in the halo mass function is directly reflected on the high redshift galaxy luminosity function. Given that the  $L_c(M, z = 0)$  relation flattens at mass scales  $\sim 10^{13} M_\odot$  (Cooray & Milosavljević 2005a), the rapid decline in the number density of massive halos, corresponding to groups and clusters, does not lead to the same fractional decline in the bright-end of the galaxy LF, relative to values today. However, models based on the evolution of the mass function alone suggest a decline in the density of bright galaxies at high-redshifts when compared to densities measured today.

On the other hand, the observed galaxy LF at high redshifts indicates that the bright-end density is, in fact, increasing as one moves to  $z \sim 3$  from today. To compensate for the decline in the number density of dark matter halos that host galaxies, associated with the redshift evolution of the mass function, the only possibility to increase the density of luminous galaxies is to consider positive luminosity evolution; the galaxies *must* brighten at high redshifts relative to luminosity values today. This brightening can be accomplished in several ways: First, galaxies, regardless of the host halo mass, can brighten by a constant factor; This description can be considered as a scenario involving pure luminosity evolution. We consider this possibility by scaling the  $L_c(Mz, z = 0)$  relation by  $(1+z)^\alpha$ . With  $\alpha = 0.75$ , our model descriptions are plotted in Figure 3. For comparison, we also plot the measured LFs by Giallongo et al. (2005) where we show the total sample as well as the division to galaxy types. The  $L_c(M, z)$  relations related to this pure luminosity evolution scenario is shown in Figure 1(a). The model can provide an adequate description, though one underestimates the density of most luminous galaxies shown with the bright-end data points in Figures 3(b), (c) and (d), while overestimating the faint-end density, for example, in Figure 3(c). To obtain a better fit to the bright-end density, one can increase  $\alpha$ . This, however, comes at the expense of overestimating the number density of galaxies at the faint-end further.

A better description of the Giallongo et al. (2005) data may be that the luminosity evolution is mass dependent. In Figure 1(b), we plot  $L_c(M, z)$  relations under this alter-

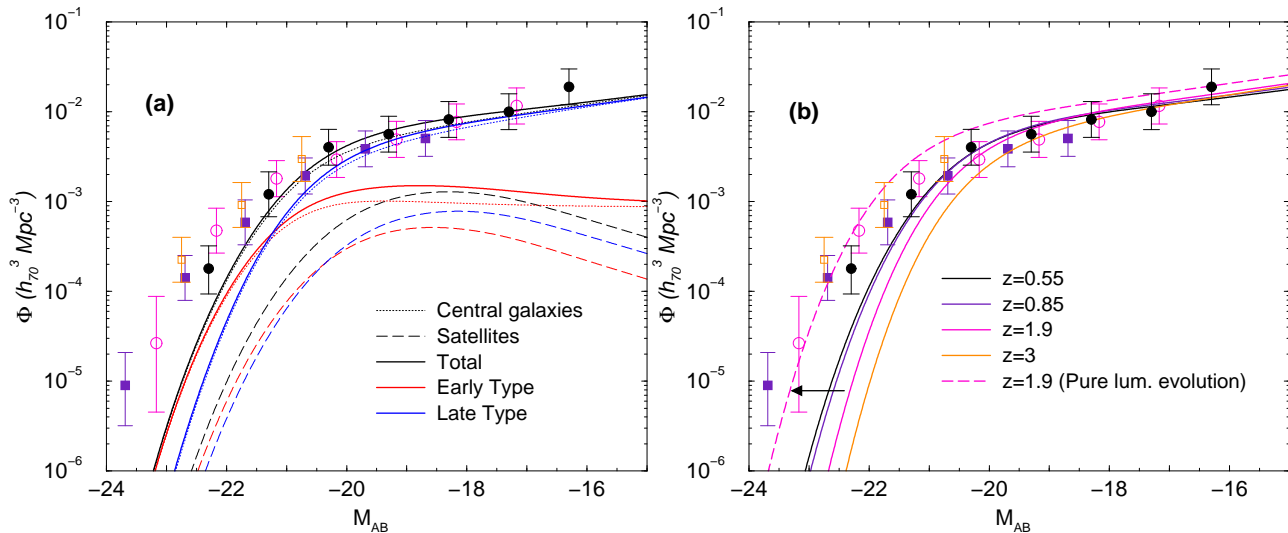


**Figure 2.** The LF of galaxies. In both panels, the data shown are the total LF from Giallongo et al. (2005) corresponding to redshifts between 0.4 and 0.7 (filled circles), 0.7 to 1.0 (open circles), 1.3 to 2.5 (filled squares) and 2.5 to 3.5 (open squares). In (a), the plotted curves are the LF at  $z = 0$  divided to central galaxies (dotted lines), satellites (dashed lines), and the total (solid line). We also further subdivide the sample to early (red lines) and late type (blue lines) galaxies, based on the model description of Cooray (2005). Note that the high- $z$  LF, when compared to  $z \sim 0$ , shows an increase in the number density at the bright end, while the faint-end density remains the same. In (b), we show the expected LF at the mid redshift of redshift ranges considered in Giallongo et al. (2005) and under the assumption that  $L_c(M, z) = L_c(M, z = 0)$ ; the resulting redshift variations are associated with evolution of the dark matter halo mass function (see, e.g., Reed et al. 2003). A simple modification under the assumption of a pure luminosity evolution, a constant shift in magnitude, as shown by a long-dashed line, cannot describe the high-redshift LF. In the CLF-based approach, since the halo mass function at the high-mass end decreases as the redshift is increased, the increase in the bright-end density could only be associated with an increase in the luminosity of galaxies, for a given halo mass. To avoid increasing the faint-end density, however, the increase in luminosity should only be associated with dark matter halos with masses corresponding to the bright-end of the LF.

native description, where we allow the luminosity of halos above the flattening mass scale to grow rapidly with redshift. This is accomplished with two parameters  $\beta$  and  $\eta$ , though, alternative model descriptions that increase luminosities of central galaxies in massive dark matter halos, while keeping the luminosity at the low-end of the mass distribution essentially the same as today, can also be considered. As shown in Figure 4, with the mass-dependent luminosity evolution description, the density of bright galaxies is increased while keeping the faint-end density similar to values measured out to  $z \sim 3$ . It is likely that this model provides a more accurate description of the data, though given various uncertainties in LFs out to a redshift of 3.5, we cannot distinguish reliably between the mass-dependent luminosity evolution and the pure luminosity evolution description.

In addition to the redshift evolution of the total galaxy LF, the model description following Cooray (2005) is also in good agreement with high redshift LFs of galaxy types. Note that we have assumed no redshift variation in the fraction of red and blue galaxies, as a function of the halo mass, between now and redshifts out to 3.5. As shown in Figures 3 and 4, these models generally overestimate the LF of red galaxies at the faint-end, while the disagreement is lower with the mass-dependent luminosity evolution scenario. At  $z > 1$ , the fraction of blue galaxies increases; in Cooray (2005), the late-type (blue) fraction of central galaxies increases at low-mass halos. Thus, at high redshifts, with the

rapid disappearance of halos with masses above few times  $10^{13} M_\odot$ , the blue fraction begins to dominate. This, however, does not mean that all galaxies at redshifts out to 3.5 is late-types. We certainly expect  $\sim 50\%$  of bright galaxies at redshifts  $\sim 3$  to be early type, red galaxies. The exact observed fraction of late- vs. early-type galaxies, as a function of redshift, can eventually be used to update the model description in Cooray (2005), especially to understand whether there is a redshift evolution in the galaxy type fraction relative to values seen today. A lack of an evolution in the blue, or red, galaxy fraction, as a function of halo mass, may support approaches such as the halo model, where galaxy properties are expected to be dependent only on mass and not the environment, though, this assumption should certainly break down near the epoch of initial galaxy formation.

### 3.1 $z \sim 6$ LF

While there is no measured LF of galaxies at  $z \sim 6$  in the rest B-band, ignoring complications resulting from differences in the rest wavelength, we can also compare our model predictions with the UV LF at  $z \sim 6$  from Bouwens et al. (2004a). In Figure 5, we summarize our results. Note that the pure luminosity evolution scenario over predicts the LF at all luminosities of interest, while the mass-dependent luminosity evolution provides a reasonable description of the data; note that any agreement or disagreement between these models

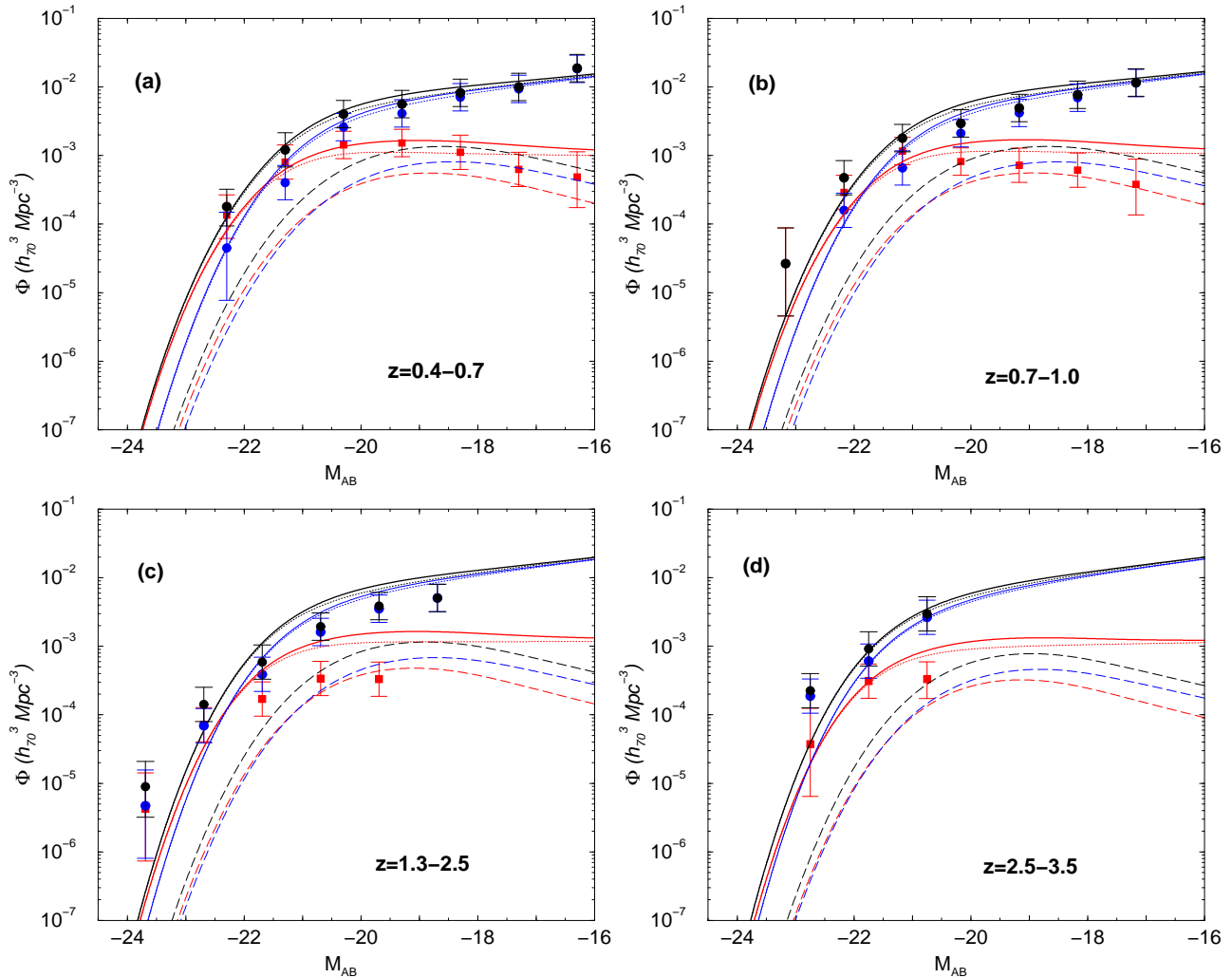


**Figure 3.** Luminosity function in the B-band as a function of redshift. From (a) to (d), we show the LF in four redshift ranges considered by Giallongo et al. (2005) with (a) 0.4 to 0.7, (b) 0.7 to 1.0, (c) 1.3 to 2.5, and (d) 2.5 to 3.5. In addition to the total LF, we also show the division to red and blue galaxies. The plotted curves are predictions based on the luminosity evolution shown in Figure 1(a), with  $L_c(M, z) = L_c(M, z = 0)(1 + z)^{0.75}$ . The lines follow Figure 2(a), with dotted lines for central galaxies, dashed lines for satellites, and solid lines for the total sample. The red lines are for the red galaxy LF and the blue lines show the blue galaxy LF. We will use this line conventions through out the paper when we plot the LF.

and measurements must be considered with the difference in color in mind. This is due to the fact that, while the  $L_c(M, z = 0)$  relation is constructed as appropriate for the B-band, the measurements at  $z \sim 6$  is in the rest UV band. Given differences in model predictions compared to measurements in Figure 5, however, we believe that the two luminosity evolution descriptions, pure luminosity evolution at all mass scales or mass-dependent luminosity evolution only at the high mass end, may be distinguished with  $z \sim 6$  LFs, though these two models give equally acceptable description of LFs out to a redshift of 3.5. Thus, based on the UV LF at  $z \sim 6$ , we suggest that a favorable description of the high-redshift galaxies may be the evolution of luminosities based on the host halo mass. As shown in Figure 5, the LF is clearly dominated by late-type blue galaxies. The early-type red galaxies will only appear, in the statistical sense,

at the bright-end with a density close to that of blue galaxies. At the faint-end, for each red-type galaxy, one should statistically expect a factor of 5 to 10 more blue galaxies, depending on the luminosity.

Given that our model for the LF is constructed from CLFs — the number of galaxies as a function of the halo mass — we can directly address an important question as to what mass dark matter halos host galaxies seen at  $z \sim 3$  to 6. We show the mass dependence of the LF in Figure 6. At  $z \sim 3$ , galaxies that are brighter than  $M_{AB} \sim -22$  are hosted in dark matter halos with masses in the range of  $10^{12}$  to  $10^{13} h_{70}^{-1} M_{\odot}$ . To statistically detect dark matter halos at  $\sim 10^{11} M_{\odot}$ , one must study the LF down to an absolute magnitude of -18. In the case of  $z \sim 6$  galaxy LF, all galaxies in the luminosity range corresponding to absolute magnitudes between -22 and -19 are hosted in dark matter

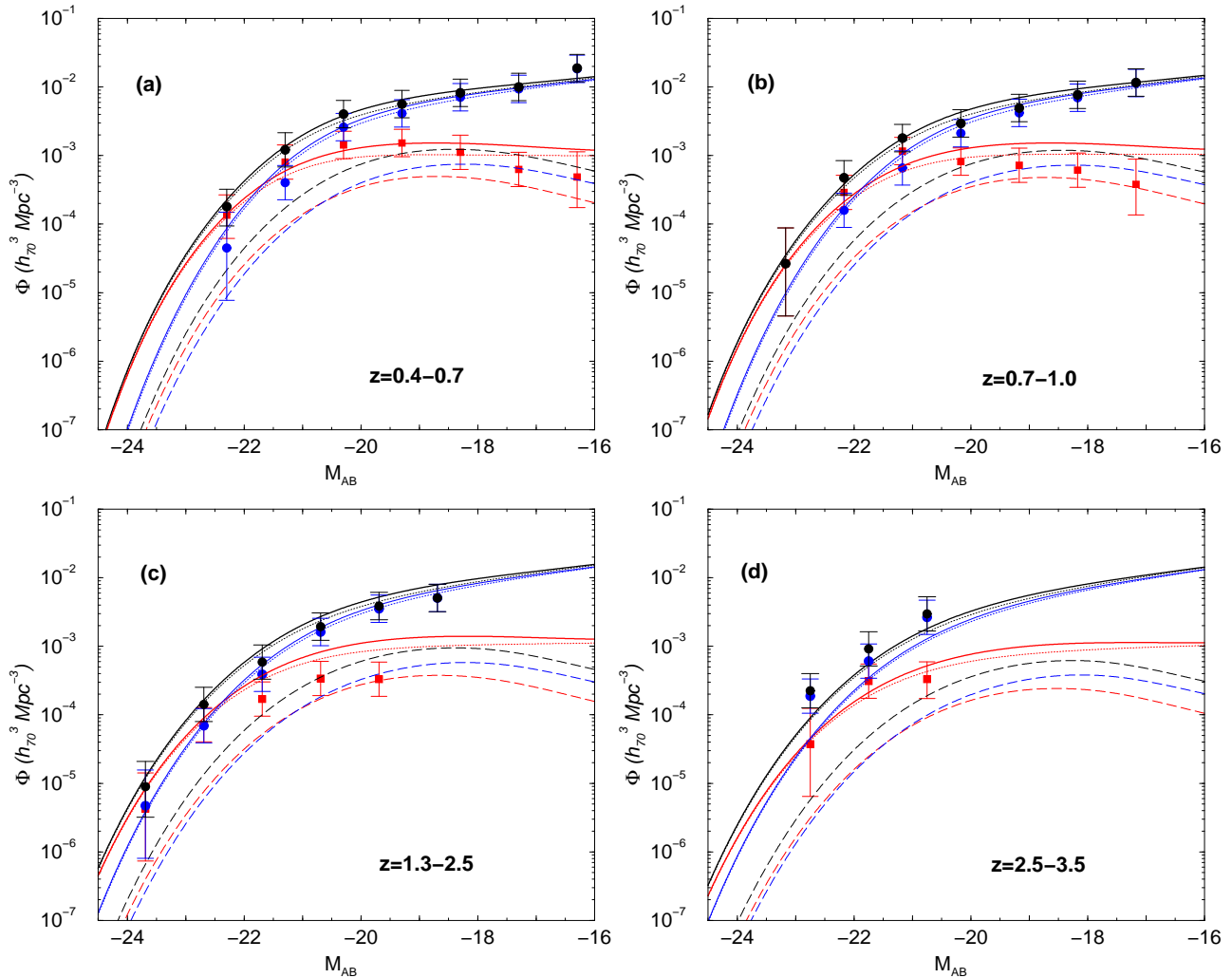


**Figure 4.** Luminosity function in the B-band as a function of redshift. The figure is same as Figure 3, except that the plotted curves are the prediction based on the mass dependent luminosity evolution shown in Figure 1(b).

halos between  $10^{11}$  to  $10^{12} h_{70}^{-1} M_{\odot}$ ; the bright-end of the  $z \sim 6$  LF corresponds to the upper-end of this mass range.

While these are approximate mass ranges, using CLFs, we can quantify the mass distribution of  $z \sim 3$  to 6 galaxies exactly. Here, we calculate the conditional probability distribution  $P(M|L, z)$  that a galaxy of a given luminosity  $L$  at redshift  $z$  is in a halo of mass  $M$  (Yang et al. 2003b, Cooray 2005):

$$P(M|L, z)dM = \frac{\Phi(L|M, z)}{\Phi(L, z)} \frac{dn(z)}{dM} dM. \quad (4)$$

In Figure 7, we summarize our results, where we plot probabilities at luminosities that correspond to absolute magnitudes of -18 to -24. At the bright end of  $M_{AB} = -24$ , at  $z \sim 3$ , galaxies are primarily in dark matter halos of mass  $\sim 10^{13} M_{\odot}$ . In comparison, such galaxies are central galaxies in groups and clusters today with masses above  $10^{14} M_{\odot}$ . At  $z \sim 6$ ,  $M_{AB} = -24$  galaxies are primarily in dark matter halos with mass  $\sim 5 \times 10^{12} M_{\odot}$ . Similarly,  $M_{AB} = -18$  galaxies at  $z \sim 3$  are found in dark matter halos with mass

$10^{11} M_{\odot}$ , though one finds a few percent probability that some of these galaxies are satellites of dark matter halos with masses between  $10^{12} M_{\odot}$  and  $10^{13} M_{\odot}$ . The four panels, when combined, show the mass-dependent redshift evolution of the galaxy luminosity. Luminous galaxies at high redshifts are found at lower mass halos than dark matter halo masses that corresponds to the same galaxy luminosity today. At the faint-end,  $M_{AB} > -20$ , regardless of the redshift, faint galaxies are essentially found in dark matter halos with a similar range in mass, though at low redshifts, a 30% or more fraction of low-luminous galaxies could be satellites in more massive halos.

While we have simply used the LF to establish the mass scale of  $z \sim 3$  to 6 galaxies, previous attempts have also been made to establish the dark matter halo masses associated with these galaxies. These estimates on halo masses were primarily based on observed galaxy clustering at these redshifts (e.g., Steidel et al. 1998; Bullock et al. 2002; Moustakas & Somerville 2002). To compare with these halo mass

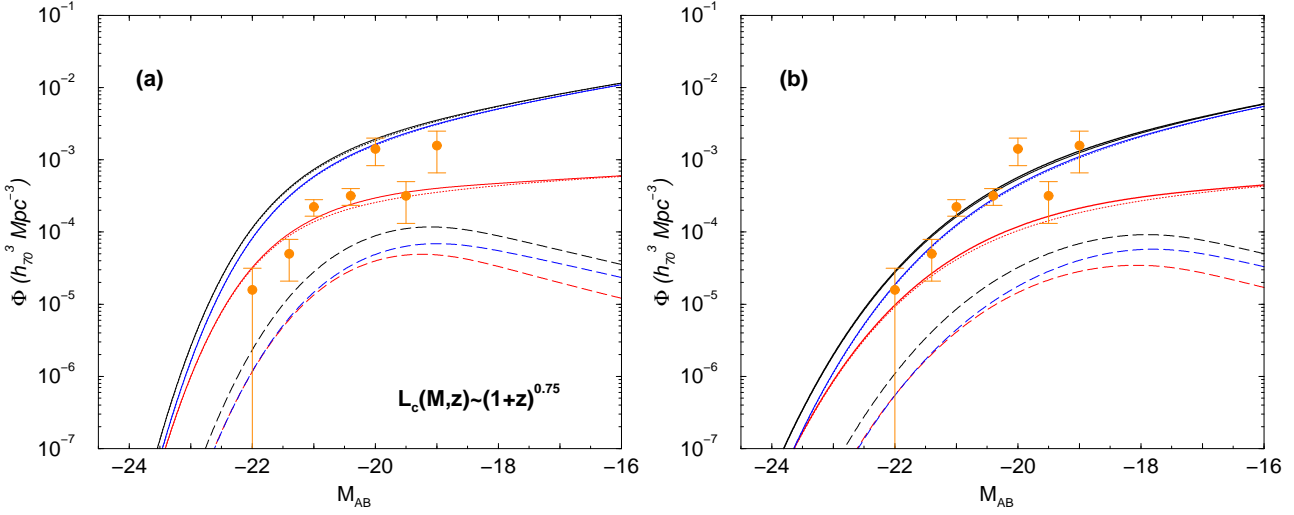


**Figure 5.** The  $z \sim 6$  UV LF. The measurements are from Bouwens et al. (2004a). The curves show the model prediction based on pure-luminosity evolution, in panel (a), and mass-dependent luminosity evolution, in panel (b), following Figure 1. The lines follow the color and style scheme used in Figure 2. As shown in (a), pure luminosity evolution matched to describe LFs out to  $z \sim 3$  overestimates the observed density of galaxies, while a mass-dependent luminosity evolution can provide an adequate description. Note that there is a slight complication in this comparison; the measurements are in the rest UV band while the predictions are based on a  $L_c(M, z = 0)$  relation that is appropriate for rest B-band.

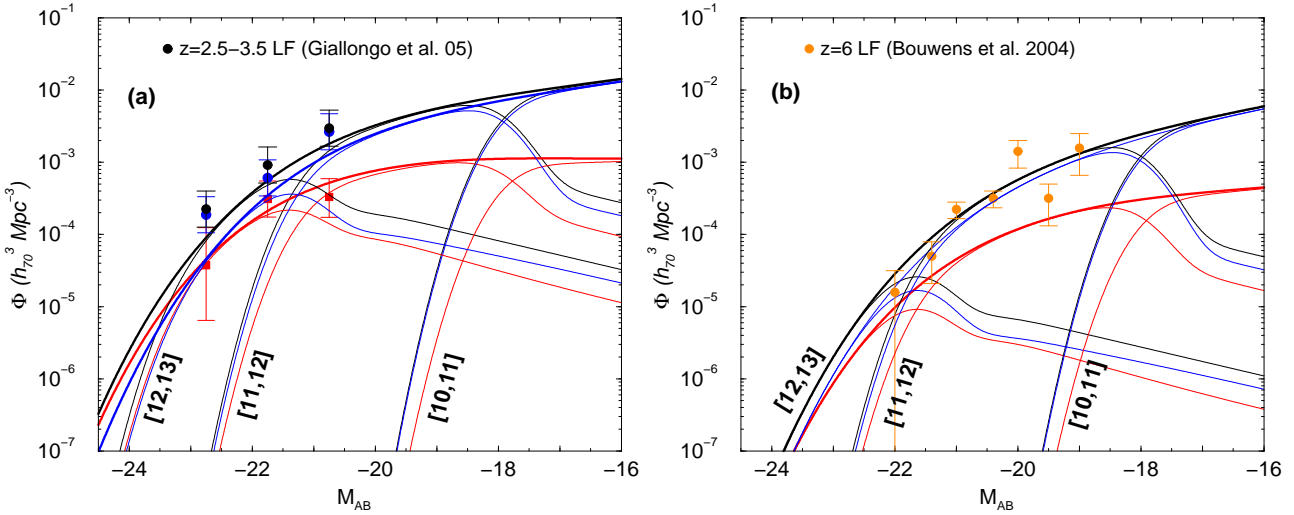


**Figure 6.** The mass dependence of the LF. In (a), we consider the  $z \sim 3$  rest B-band LF from Giallongo et al. (2005), while in (b), we consider the  $z \sim 6$  rest UV LF from Bouwens et al. (2004a). In both panels, the plotted curves are for the mass-dependent luminosity evolution considered in Figure 4 (and show in Figure 1b). The mass ranges, in logarithmic values, are labeled on these plots. The  $z \sim 3$  LF is dominated by galaxies in dark matter halos between  $10^{11}$  to  $10^{13} M_{\odot}$ , while the  $z \sim 6$  LF is dominated by dark matter halos between  $10^{11} M_{\odot}$  and  $10^{12} M_{\odot}$ .

estimates, which essentially lead to an estimate of the average halo mass, we calculate the probability distribution of halo mass associated with high-redshift galaxies:

$$P(M|z)dM = \frac{\int_{L_{\min}} dL \Phi(L|M, z) \frac{dn(z)}{dM}}{\int_{L_{\min}} \Phi(L, z)} dM, \quad (5)$$

with the low-end of luminosity integral set at  $L_{\min}$ . For example, to compare with Moustakas & Somerville (2002) estimate on the average  $z \sim 3$  Lyman Break Galaxy (LBG) halo

mass, we set  $L_{\min}$  to be that corresponding to  $M_{AB} \sim -20.8$ ; at this magnitude level, the number density of  $z \sim 3$  galaxies is  $\sim 5 \times 10^{-3} h^3 \text{ Mpc}^{-3}$ , comparable to the number density of LBG galaxies used in Moustakas & Somerville (2002) together with clustering statistics (correlation length and bias) of galaxies down to this density.

Figure 8 shows the probability distribution of mass related to this number density of galaxies at  $z \sim 3$ . The probability peaks around  $\sim (6 \text{ to } 9) \times 10^{11} h^{-1} M_{\odot}$ , which is

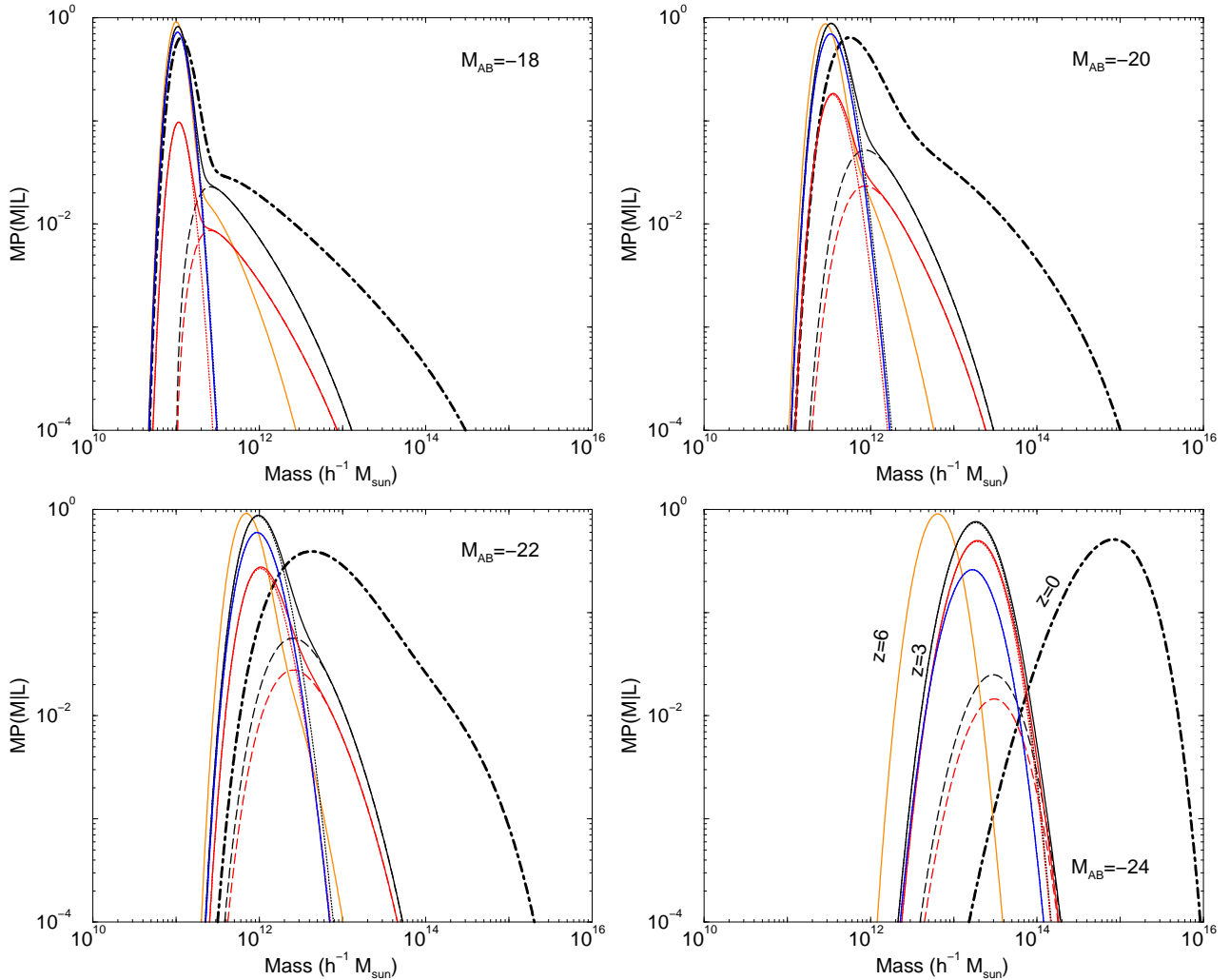


**Figure 7.** The conditional probability distribution function of halo mass  $P(M|L)$  to host a galaxy of the given luminosity at a redshift of 3, as a function of the halo mass. The black lines are the total galaxy sample, while red and blue lines show the sample divided to early- and late-type galaxies. The probabilities are calculated for the mass-dependent luminosity evolution model. From top-left to bottom-right, we show these probabilities for  $M_{AB} = -18, -20, -22,$  and  $-24$ , respectively, in the B-band. The thick dot-dashed line is the same probability distribution for the total galaxy sample at  $z = 0$ , while the orange line shows the same at  $z = 6$ .

roughly consistent, though slightly higher than, the average halo mass of  $5.5 \times 10^{11} h^{-1} M_{\odot}$  suggested in Moustakas & Somerville (2002). While the approach based on galaxy clustering allows the average halo mass scale to be established, making use of CLFs, here, we have quantified the dark matter halo mass of  $z \sim 3$  and 6 galaxies as a probability distribution function.

In Figure 9, we compare our predictions with several measurements in the literature on the UV LF at high redshifts. At  $z \sim 3$ , Lyman-break galaxy (LBG) LF is measured by Steidel et al. (1999). We find reasonable agreement, though we emphasize that our models are constructed for the rest B-band instead of rest UV-band related to these observations. For reference, we also show the LF of galaxies at redshifts 8 and 10; while no measurements currently exist at these high redshifts, the agreement, at least out to  $z \sim 6$  suggests that our predictions may be directly testable in the

near future using deep IR images in near-IR wavelengths. Relative to  $z \sim 6$  LF, the  $z \sim 10$  LF predicts a factor of  $\sim 10$  lower number density of galaxies at  $M_{AB} \sim -20$ . Based on  $i$ -band dropouts, the surface density of  $z \sim 6$  galaxies, is roughly  $\sim 0.5 \pm 0.2$  galaxies per square arcmin. To detect a  $z \sim 10$  galaxy, it may be that one must search over an area of  $\sim 15$  to 30 square arcmins, on average. The strong clustering of high- $z$  galaxies, discussed below, may affect search for these galaxies.

In Figure 10, for comparison with existing measurements, we plot the cosmic luminosity density as a function of redshifts. These luminosity densities are calculated via  $\rho_L(z) \propto \int_{L_{\min}} L \Phi(L, z) dL$ , where we consider two values for the minimum luminosity. In Figure 10(a), we consider a fainter cut off, at  $M_{AB} \sim -16$ , and compare with measurements of the luminosity density at rest B-band from the literature. Our predictions generally agree at low redshifts,

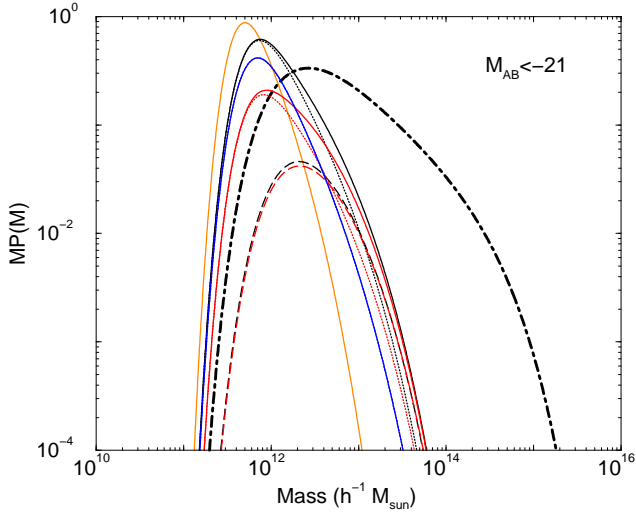


**Figure 8.** The probability distribution function of halo mass  $P(M, z = 3)$  hosting galaxies down to number density of galaxies of  $\sim 5 \times 10^{-3} h^3 \text{ Mpc}^{-3}$  at  $z = 3$ . For comparison, we also show the same distribution, down to the same luminosity, at today (dot-dashed line), and at a redshift of 6 (solid-orange line). The probability distribution peaks around a mass of  $7 \times 10^{11} h^{-1} M_{\odot}$  and is consistent with the average LBG halo mass determined by Moustakas & Somerville (2002) based on the clustering properties of galaxies down to the same number density of galaxies.

though, over predicts the density measured by Dahlen et al. (2005) using LFs constructed from GOODS data. In Figure 10(b), we set the low luminosity end of the integral to be roughly  $0.3L_{\star}$  ( $M_{\text{AB}} \sim -20$ ) at  $z \sim 3$  to be consistent with most measurements by Bouwens et al. (2004a, 2004b, 2005). In this panel, we compare with measurements of the luminosity density at high redshifts in the rest UV-band. Note that our underlying model here is designed for rest B-band and we do not attempt to include any corrections due to color differences when comparing with observations at rest UV wavelengths. Our models suggest that the luminosity density at  $z \sim 10$  should be an order of magnitude below what is suggested in Bouwens et al. (2005), under the assumption that they detect 3  $z \sim 10$  dropouts in deep HST NICMOS fields in a search area over  $z \sim 15$  square arcmins. Based on our LFs, we expect at most a single  $z \sim 10$  galaxy in such a small survey area. If a significant density of  $z \sim 10$  galaxies were to exist, one would require a sharp increase in the evolution of galaxy luminosities at halo mass scales around  $\sim 10^{11} M_{\odot}$  than the luminosity evolution we have suggested so far to explain  $z \sim 3$  to 6 galaxy LFs.

### 3.2 Galaxy Bias

While our models can generally describe the LF of galaxies at redshifts out to 6, another useful quantity to compare with observed data is the galaxy bias, as a function of the luminosity. Using the conditional LFs, we calculate the luminosity and redshift dependent galaxy bias as

$$b(L, z) = \int b_{\text{halo}}(M, z) \frac{\Phi_i(L|M, z)}{\Phi_i(L, z)} \frac{dn}{dM}(z) dM, \quad (6)$$

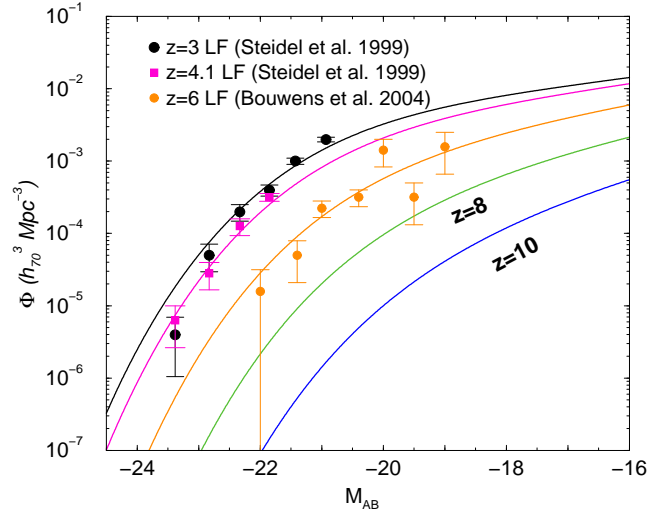


**Figure 9.** The  $z = 3$  to 10 galaxy LFs; the plotted data show the measured LFs at  $z \sim 3$  and 4.1 by Steidel et al. (1999) and at  $z \sim 6$  by Bouwens et al. (2004a). The solid lines show the expected LF (strictly speaking, in the rest B-band), as a function of redshift with redshift values chosen, from top to bottom, of 3, 4, 6, 8 and 10. The decline in the density of galaxies at redshifts greater than 3 is a reflection of the rapid decline in the number density of dark matter halos; this decrease should not be explained as an effect associated with negative luminosity evolution, since in our model, luminosities at the bright-end does evolve, though the number of halos hosting such bright galaxies is decreasing.

where  $b_{\text{halo}}(M, z)$  is the halo bias with respect to the linear density field (Sheth, Mo & Tormen 2001; also, Efstathiou et al. 1988; Cole & Kaiser 1989; Mo et al. 1997) and  $i$  denotes the galaxy type.

In Figure 11, we show the galaxy bias as a function of the luminosity. We also divide the sample to galaxy types and redshifts at  $z = 0, 3$  and 6. At redshift of 3, we plot several estimates of the LBG bias; we convert the bias–number density relations, from e.g., Bullock et al. 2002, to plot bias as a function of luminosity based on the expected number density of  $z \sim 3$  galaxies, down to the given luminosity, given our model description for the LF. The  $b(L)$  relation provides a more direct approach to compare how galaxy bias evolves with redshift, than using the bias factor as a function of the number density, though the latter is what is measured from the data; With adequate statistics, in fact, it should be possible to measure  $b(L)$  relation at high redshifts directly from the data as has been at  $z = 0$  with SDSS (Zehavi et al. 2004) and with 2dFGRS (Norberg et al. 2002b). As shown in Figure 11, the  $z \sim 6$  galaxies are biased by factors of  $\sim 3$  or higher relative to the linear density field. While there are no published measurements of galaxy clustering at  $z \sim 6$ , the existence of clustered large-scale structures has been noted through searches for Lyman- $\alpha$  emitters at these redshifts (e.g., Ouchi et al. 2005; Wang et al. 2005). While our models were developed to discuss the LF and clustering of galaxies, one can easily modify the current prescriptions to describe statistics of sources such as Lyman- $\alpha$  emitters;

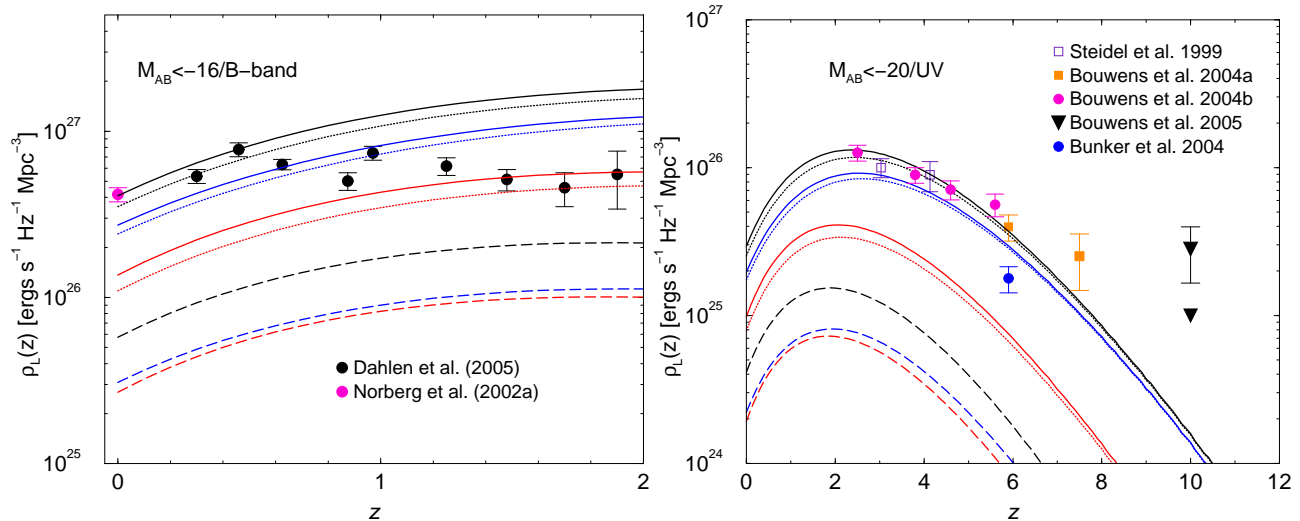


**Figure 10.** The cosmic luminosity density as a function of the redshift. The plotted curves are the expectations based on the mass-dependent luminosity evolution model. In (a), we integrate to a the faint-end magnitude and compare with predictions from the literature at rest B-bands. By design, we recover the luminosity density at  $z \sim 0$  measured from the 2dFGRS survey (Norberg et al. 2002a), though we over predict the luminosity density at redshifts  $\sim 1$  to 2 when compared to measurements by Dahlen et al. (2005). In (b), we consider a brighter cut off in luminosity chosen to be roughly consistent with the cut-off in the measured luminosity densities by Bouwens et al. (2004a). Now, we compare with measurements at high redshifts in the rest-UV wavelengths (see, figure panel for references). In converting to UV luminosity densities, we have ignored any color corrections resulting from the  $L_c(M, z)$  relation designed to model rest B-band LFs.

we plan to model Ly- $\alpha$  galaxy statistics at redshifts 4 to 7 in an upcoming paper.

#### 4 SUMMARY AND CONCLUSIONS

To summarize our discussion involving high-redshift galaxy LFs, our main results are:

(1) Galaxy luminosities must evolve with redshift; while to describe rest B-band LFs out to  $z \sim 3$ , one can consider either a mass-independent evolution, with luminosities increasing as  $(1+z)^{0.75}$ , or a mass-dependent evolution scenario (see, Figure 1b); the  $z \sim 6$  galaxy LF is more compatible with a mass-dependent evolution model. In this scenario, galaxies that are present in halos above  $\sim 10^{12} M_\odot$  brighten by factor of 4 to 6 between now and  $z \sim 6$ . This suggests that the star formation rate, per given dark matter halo mass, was increasing to high redshifts and that the star formation was more efficient in the past relative to low redshifts. A conclusion similar to what we generally suggest here was also reached by Dahlen et al. (2005) based on the rest B-band LF constructed from GOODS data.

(2) While the bright-end density of galaxies increases with redshift, the faint-end density remains essentially the same out to  $z \sim 3$ . The suggested evolution in then  $L_c(M)$  relation with redshift compensates for the decrease in dark matter halo density. Another important reason why the number density of bright galaxies does not decrease rapidly out to a  $z \sim 2$  is that  $L_c(M)$  relation flattens at a halo mass scale around  $10^{13} M_\odot$ ; at low redshifts, the redshift evolution of the dark matter halo mass function mostly results in a decrease in the number density of massive halos,

while the number density around  $10^{13} M_\odot$  is not affected. At  $z > 2$ , the exponential cut-off associated with the halo mass function moves to mass scales around and below  $10^{13} M_\odot$ . This leads to a decrease in the number density of halos hosting central galaxies over the range in luminosity of interest. Thus, the turn over in the LF at the bright-end between redshifts 2 to 3 is a reflection on the lack of an adequate density of dark matter halos with masses around  $10^{13} M_\odot$  to host bright galaxies. One does not need to involve different or multiple scenarios to explain why the density of bright galaxies first increases and then decreases at redshifts greater than 2 to 3. Even in the presence of a decrease in the number density of bright galaxies as a function of redshift, the suggested luminosity evolution continues to be present.

(3) The mass scale of galaxies at redshifts  $\sim 3$  is distributed between  $\sim 10^{11} M_\odot$  to  $10^{12} M_\odot$  (Figure 8). The bright galaxies at  $z \sim 3$  (with  $M \sim -24$ ) are found in dark matter halos with masses around  $10^{13} M_\odot$ . Today, these galaxies are found in dark matter halos with masses around  $10^{15} M_\odot$ , or as central galaxies in massive clusters. At a redshift of  $\sim 6$ , these galaxies were in dark matter halos of mass few times  $10^{12} M_\odot$ .

(4) The number density of  $z \sim 10$  galaxies are roughly a factor of 10 lower than the density of galaxies at  $z \sim 6$ ; if a higher density is found, the  $L_c(M, z)$  relation must evolve rapidly at redshifts above 6 than suggested here to explain  $z \sim 3$  to 6 LFs. If our predictions our correct, one must search roughly an area of  $\sim 30$  sq. arcmins to find a galaxy at a redshift of 10. The high redshift galaxies are extremely biased with respect to the linear dark matter density field; the bias factor of galaxies at  $z \sim 6$  varies from less than

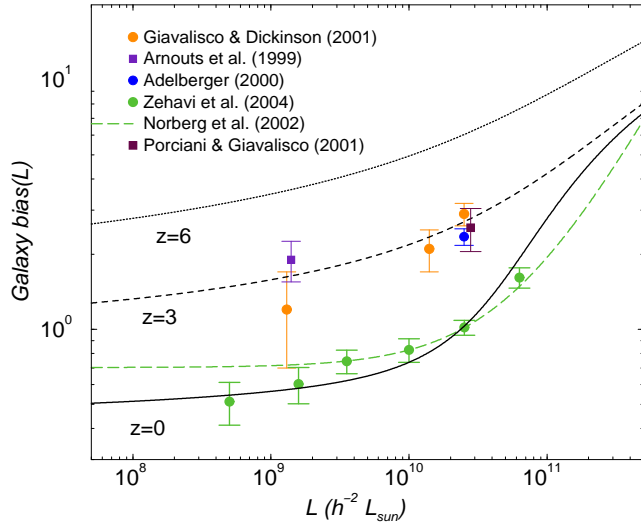


**Figure 11.** The galaxy bias as a function of luminosity. We show bias measurements at  $z = 0$  in SDSS (Zehavi et al. 2004) and with 2dFGRS (Norberg et al. 2002b). The  $z \sim 3$  bias values come from the literature; we have converted the LBG number density and bias relations (e.g., Bullock et al. 2002) to luminosity–bias relation based on the expected number density of galaxies down to a certain luminosity using the predicted LF of galaxies at  $z \sim 3$ . We also show a precision related to the expected clustering bias of galaxies at  $z \sim 6$ ; at this redshift, galaxies are significantly biased with typical bias values  $\sim 3$ .

3 to 10 for brightest galaxies. Our predictions for clustering bias factors, as a function of luminosity, are in general agreement with estimated values based on the correlation length (Figure 11), at least out to  $z \sim 3$ .

To conclude, we have presented a description of the LF of galaxies as a function of redshift, in the rest B-band, using a simple empirical model. The approach has the main advantage that one can extract underlying reasons associated with the observed evolution of the LF. Here, we have characterized this evolution in terms of the  $L_c(M, z)$  relation — the luminosity of central galaxies of dark matter halos as a function of halo mass and redshift. Given the rapid decline in the number density of dark matter halos, in order to explain the presence of bright galaxies, we have suggested that the  $L_c(M, z)$  relation must evolve such that galaxies have a higher luminosity, when compared to today, at the high mass end of the halo distribution.

The  $z = 0$ ,  $L_c(M)$  relation was explained in Cooray & Milosavljević (2005a) in terms of dissipationless merging of galaxies in dark matter halos centers. The flattening of the  $L_c(M)$  relation at halo mass scales  $\sim 10^{13} M_\odot$  was suggested as due to a decrease in the efficiency at which dynamical friction decays satellite orbits to merge with the central galaxy; the dynamical friction time scale for the merging of satellites in halos with masses above few times  $10^{13} M_\odot$  is more than Hubble time. As one moves to a high redshift, the flattening mass scale is expected to move to a lower mass scale given that the age of the Universe, or the age of the halo since it formed, is lower than the age today. Such a behavior is captured in our empirical model for the  $L(M, z)$  relation

based on mass-dependent luminosity evolution. While our approach has allowed us to capture the evolution associated with the  $L_c(M, z)$  relation, what physical processes govern this behavior is yet to be understood. Any reasonable explanation for the brightening of galaxies at high redshifts must consider the merging history in addition to the underlying astrophysical reason why galaxies were brighter in the past when compared to today. The  $L_c(M, z)$  relation is certainly a key aspect in galaxy formation and evolution, and we expect approaches involving numerical simulations (e.g., Kay et al. 2002) and semi-analytic models (e.g., Benson et al. 2003) will be used to understand if what we have suggested on the evolution of this relation is consistent or not with astrophysical processes associated with galaxy formation and evolution.

*Acknowledgments:* The author thanks Emanuele Giallongo for electronic tables of the high-redshift LFs and members of Cosmology and Theoretical Astrophysics groups at Caltech and UC Irvine for useful discussions.

## REFERENCES

- Benson, A. J., Pearce, F. R., Frenk, C. S., Baugh, C. M., & Jenkins, A. 2001, *Mon. Not. R. Astron. Soc.*, 321, L7
- Berlind, A. A., Weinberg, D. H., Benson, A. J. et al. 2003, *Astrophys. J.*, 593, 1
- Bouwens, R., Illingworth, G. D., Thompson, R. I. et al. 2004a, *Astrophys. J.*, 606, L25
- Bouwens, R., Thompson, R.I., Illingworth, G. D. et al. 2004b, *Astrophys. J.*, 616, L79
- Bouwens, R., Illingworth, G. D., Thompson, R. I. & Franx, M. J. 2005, *Astrophys. J.*, 624, L5
- Bullock, J. S., Wechsler, R.S., & Somerville, R. S. 2002, *Mon. Not. R. Astron. Soc.*, 329, 246
- Bunker, A. J., Stanway, E. R., Ellis, R. S. & McMahon, R. G. 2004, *Mon. Not. R. Astron. Soc.*, 355, 374
- Coil, A. L. et al. 2004, *Astrophys. J.*, 609, 525
- Cole, S. & Kaiser, N. 1989, *Mon. Not. R. Astron. Soc.*, 237, 1127
- Colless, M. et al. 2001, *MNRAS*, 328, 1039
- Cooray A., Hu W., & Miralda-Escudé, J. 2000, *Astrophys. J.*, 535, L9
- Cooray A. 2002, *Astrophys. J.*, 576, L105
- Cooray, A., & Sheth, R. 2002, *Phys. Rep.*, 372, 1 (astro-ph/0206508)
- Cooray, A., & Milosavljević, M. 2005a, *ApJ* in press (astro-ph/0503596)
- Cooray, A., & Milosavljević, M. 2005b, *ApJ* in press (astro-ph/0504580)
- Cooray, A. 2005, *Mon. Not. R. Astron. Soc.* submitted (astro-ph/0505421)
- Dahlen, T., et al. 2005, *Astrophys. J.* in press (astro-ph/0505297)
- De Lucia, G., Kauffmann, G., Springel, V., White, S. D. M., Lanzoni, B., Stoehr, F., Tormen, G., & Yoshida, N. 2004, *Mon. Not. R. Astron. Soc.*, 348, 333
- Drory, N., Bender, R., Feulner, G., Hopp, U., Marston, C., Snigula, J., & Hill, G. J. 2003, *Astrophys. J.*, 595, 698
- Efstathiou, G., Frenk, C. S., White, S. D. M. & Davis, M. 1988, *Mon. Not. R. Astron. Soc.*, 235, 715
- Giallongo, E., Salimbeni, S., Menci, N. et al. 2005, *Astrophys. J.*, 622, 116
- Jenkins, A., Frenk, C. S., White, S. D. M., Colberg, J. M., Cole,

- S., Evrard, A. E., Couchman, H. M. P., & Yoshida, N. 2001, *Mon. Not. R. Astron. Soc.*, 321, 372
- Kay, S. T., Pearce, F. R., Frenck, C. S., & Jenkins, A. 2002, *Mon. Not. R. Astron. Soc.*, 330, 113
- Kravtsov, A. V., Berlind, A. A., Wechsler, R. H., Klypin, A. A., Gottlöber, S., Allgood, B., & Primack, J. R. 2004, *Astrophys. J.*, 609, 35
- Lilly, S. J., Le Fevre, O., Hammer, F. & Crampton, D. 1996, *Astrophys. J.*, 460, L1
- Lin, Y., Mohr, J. J., & Stanford, A. 2004, *Astrophys. J.*, 610, 745
- Moustakas, L. A. & Somerville, R. S. 2002, *Astrophys. J.*, 577, 1
- Norberg, P., et al. 2002a, *Mon. Not. R. Astron. Soc.*, 336, 907
- Norberg, P., et al. 2002b, *Mon. Not. R. Astron. Soc.*, 332, 827
- Oguri, M. & Lee, J. 2004, *Mon. Not. R. Astron. Soc.*, astro-ph/0401628
- Ouchi, M., Shimasaku, K., Akiyama, M. et al. 2005, *Astrophys. J.*, 620, L1
- Press, W. H., & Schechter, P. 1974, *Astrophys. J.*, 187, 425
- Reed, D., Gardner, J., Quinn, T., et al. 2003, *Mon. Not. R. Astron. Soc.*, 346, 565
- Schechter, P. 1976, *Astrophys. J.*, 203, 297
- Soccimarro R., Sheth R., Hui L., Jain B., 2001, *ApJ*, 546, 20
- Seljak, U. 2000, *Mon. Not. R. Astron. Soc.*, 318, 203
- Sheth, R. K., & Tormen, G. 1999, *Mon. Not. R. Astron. Soc.*, 308, 119
- Sheth, R. K., Mo, H. J., & Tormen, G. 2001, *Mon. Not. R. Astron. Soc.*, 323, 1
- Spergel, D. N., et al. 2003, *Astrophys. J. Supp.*, 148, 175
- Steidel, C., Adelberger, M., Dickinson, Giavalisco, M., Pettini, M. & Kellogg, M. 1998, *Astrophys. J.*, 492, 428
- Steidel, C., Adelberger, K. L., Giavalisco, M., Dickinson, M. & Pettini, M. 1999, *Astrophys. J.*, 519, 1
- Trentham, N., & Tully, R. B. 2002, *Mon. Not. R. Astron. Soc.*, 335, 712
- Vale, A., & Ostriker, J. P. 2004, *Mon. Not. R. Astron. Soc.*, 353, 189
- Wang, J. X., Malhotra, S. & Rhoads, J. E. 2005, *Astrophys. J.*, 622, L77
- Yan, R., Madgwick, D. S. & White, M. 2003, *Astrophys. J.*, 598, 848
- Yang, X., Mo, H. J., Kauffmann, G., & Chu, Y. Q. 2003a, *Mon. Not. R. Astron. Soc.*, 339, 387
- Yang, X., Mo, H. J., & van den Bosch, F. C. 2003b, *Mon. Not. R. Astron. Soc.*, 339, 1057
- Yang, X., Mo, H. J., Jing, Y. P., & van den Bosch, F. C. 2005, *Mon. Not. R. Astron. Soc.*, 358, 217
- York, D. G., et al. 2000, *Astron. J.*, 120, 1579
- Zheng, Z., et al. 2004, preprint (astro-ph/0408564)